

Mesoscopic ‘‘Rydberg’’ atom in a microwave field

Tomaž Prosen^(a) and Dima L. Shepelyansky^(b)

^(a) Physics Department, Faculty of Mathematics and Physics, University of Ljubljana, Ljubljana, Slovenia

^(b)Laboratoire de Physique Théorique, UMR 5152 du CNRS,

Université P. Sabatier, 31062 Toulouse Cedex 4, France

(Dated: November 5, 2004)

We establish analogy between a microwave ionization of Rydberg atoms and a charge transport through a chaotic quantum dot induced by a monochromatic field in a regime with a potential barrier between dot contacts. We show that the quantum coherence leads to dynamical localization of electron excitation in number of photons absorbed inside the dot. The theory developed determines the dependence of localization length on dot and microwave parameters showing that the microwave power can switch the dot between metallic and insulating regimes.

PACS numbers: 05.45.Mt, 73.50.Pz, 32.80.Rm

The dynamical localization of quantum chaos is a generic physical phenomenon induced by quantum coherence which leads to suppression of diffusive wave packet spreading originated from dynamical chaos in the classical limit (see e.g. [1] and Refs. therein). It has been first seen in numerical simulations of the kicked rotator model [2] and, later, of a more realistic system of excited hydrogen atom in a microwave field [3]. The first observation of this phenomenon was achieved in microwave ionization experiments of hydrogen and Rydberg atoms [4, 5, 6, 7] while more recent experimental progress allowed to realize the original kicked rotator model with cold atoms in laser fields and detect with them the dynamical localization of chaos [8].

For a hydrogen atom in a microwave field the diffusive excitation in energy appears only above certain field threshold where the integrability of unperturbed motion is destroyed and the classical dynamics becomes chaotic [9]. However, in certain systems the internal dynamics can be fully chaotic on an energy surface so that classically the diffusive excitation starts for arbitrary small fields. As an example of such systems we may quote complex molecules [10], Rydberg atoms in a magnetic field [11] or chaotic Sinai billiards [12]. In such systems the quantum eigenstates are chaotic and their level spacing statistics is described by the random matrix theory [10, 11, 13, 14]. The excitation of such quantum systems by a monochromatic field represents a diffusive process of one-photon absorption/emission transitions with a rate Γ which is given by the Fermi golden rule. The quantum interference effects lead to the dynamical localization of this diffusion with the localization length l_ϕ given by [15]:

$$l_\phi = 2\pi\hbar\Gamma\rho_c. \quad (1)$$

Here l_ϕ is measured in the number of photons of monochromatic field with frequency ω , ρ_c is the level density of unperturbed system and it is assumed that $\hbar\omega\rho_c > 1$ and $l_\phi > 1$. The extensive numerical simulations of a microwave ionization of internally chaotic Rydberg atoms (chaos is produced by static magnetic or

electric field) [16] showed that the relation (1) works even in extreme regimes when up to a thousand of photons is needed to ionize one atom.

The result (1) is rather general and can be used not only for atoms but also for chaotic billiards in a microwave field. In fact, during the last decade the conductance properties of such billiards realized with 2D electron gas quantum dots of micron size have been studied in great detail both experimentally and theoretically (see reviews [17, 18] and Refs. therein). In such experiments typical parameters correspond to a dot size $a \sim 1\mu\text{m}$ and electron density $n_e \sim 4 \cdot 10^{11}\text{cm}^{-2}$. Thus with the spin degeneracy the level number at the Fermi energy is $n_F = n_e\mathcal{A}/2 \approx 2000$ where the dot area is $\mathcal{A} \sim a^2$. In fact these values of a and n_F correspond to those of a Rydberg atom with the principal number $n \sim 100$ when $a \sim n^2a_B \sim 0.5\mu\text{m}$ and $n_F \approx n^2/2 \sim 5000$. Here a_B is the Bohr radius and we keep in mind that for a linearly polarized microwave field the magnetic quantum number m_z is preserved (we assume $m_z \sim 1$). Therefore, a quantum dot with the above parameters can be viewed as a mesoscopic ‘‘Rydberg’’ atom and the process of microwave excitation of electrons should have similarities with microwave ionization of Rydberg atoms. The ionization barrier can be realized by an energy difference U between income/outcome leads so that the microwave field will switch the dot conductance from insulating (at $\hbar\omega l_\phi \ll U$) to metallic (at $\hbar\omega l_\phi > U$) regime.

To understand in a better way the requirements for microwave parameters we note that for the 2D electron gas the Fermi momentum p_F and energy E_F are given by $p_F^2 = 2\pi n_e\hbar^2$ and $E_F = p_F^2/2m$ with $m = 0.067m_e$ for $n\text{GaAs}$. The average level spacing in the dot is $\Delta = 1/\rho_c = E_F/n_F = 2\pi\hbar^2/m\mathcal{A}$. For the typical values of a and n_e used above we obtain $E_F \sim 100K$, $\Delta \sim 0.05K$ with the Fermi velocity $v_F = p_F/m \sim 2 \cdot 10^7\text{cm/s}$. Hence, the collision frequency is $\nu_c/2\pi = v_F/2a \sim 100\text{GHz}$ that is much larger than the frequency corresponding to one level spacing $\Delta/(2\pi\hbar) \sim 1\text{GHz}$. Thus for a microwave field with $\omega/2\pi < 100\text{GHz}$ *ac*-driving is in the classical

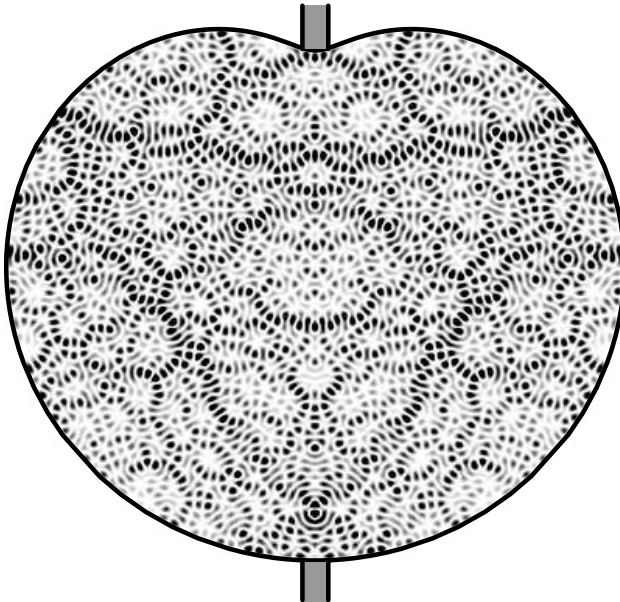


FIG. 1: Dot billiard at $\lambda = 3/8$ with the probability density of the eigenstate at the Fermi level $n_F = 2001$ (see text); density is proportional to color (white for zero, black for maximum). Dashed stripes show schematically income (bottom) and outcome (top) leads which have energy difference U .

adiabatic regime and according to the adiabatic theorem the energy excitation is exponentially small for dot billiards with integrable dynamics. However, for dots with chaotic dynamics a microwave field with $\hbar\omega > \Delta$ leads to diffusive excitation in energy E with the rate $D_E = (\delta E)^2/\delta t \approx \hbar^2\omega^2\Gamma$. For the field linearly polarized along y -axis we have $\partial E/\partial t = \epsilon\omega y \cos\omega t$ and $D_E \sim (\epsilon\omega)^2/\nu_c$ where ϵ is the field strength multiplied by the electron charge. This gives

$$l_\phi \approx 2\pi\chi\epsilon^2a^2/(\hbar\nu_c\Delta) \approx 16\chi\epsilon^2(\mathcal{A}/\mathcal{A}_0)^{5/2}(n_{e0}/n_e)^{1/2} \quad (2)$$

where χ is a numerical constant and in the right part $\mathcal{A}_0 = 1\mu m^2$, $n_{e0} = 4 \cdot 10^{11} cm^{-2}$ and ϵ is measured in V/cm . It is also convenient to write (2) in the form $l_\phi \approx \chi(\epsilon a/E_F)^2 n_F^{3/2}$ which shows that l_ϕ may be large even when $\epsilon a \ll E_F$.

To check the validity of the above estimates and obtain all numerical coefficients we study numerically the dynamical photonic localization in the billiard which is given by a conformal quadratic map of a unit circle proposed by Robnik [19]. Its shape in polar coordinates is $r(\phi) = R(1 - 2\lambda \sin \phi)$ with a parameter $\lambda \in [0, 1/2]$. For $\lambda > 1/4$ the billiard is non-convex and almost fully chaotic, while for $\lambda = 1/2$ it is rigorously known to be ergodic and belongs to the class of K-systems [12]. We restrict our studies mainly to the case with $\lambda = 3/8$ shown in Fig. 1. For the quantum evolution we consider only even states of the billiard. These states are symmetric

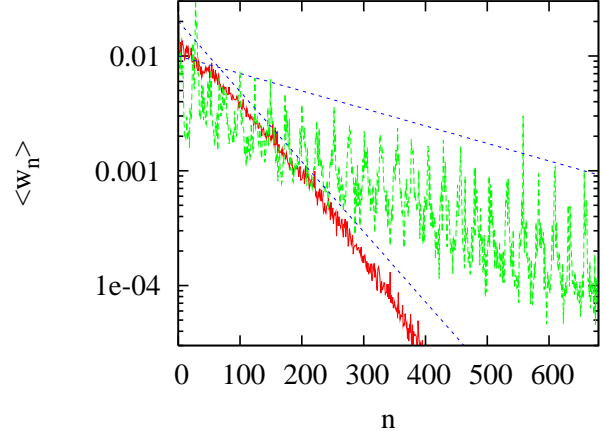


FIG. 2: (color online) Probability distribution $\langle w_n \rangle$ over the billiard eigenstates n after a pulse of 2000 microwave field periods (averaged over last 500 periods, n is counted from the Fermi level n_F). Here $\epsilon = 1200$, $\omega = 20$ (red/black curve) and $\epsilon = 300$, $\omega = 160$ (green/gray curve). Initially all probability is in the state $n = 0$ shown in Fig. 1. The straight dotted lines show the theoretical exponential decay with the localization length (3).

with respect to reflection transformation x to $-x$ and a microwave field linearly polarized along y -axis gives transitions only inside this symmetry class. We take the Fermi level to be $n_F = 2001$ in this symmetry class (total quantum number around 4000) that corresponds to $E_F = v_F^2/4 = 12586.2$ where for numerical simulations we use the usual billiard units with $\hbar = R = 2m = 1$. Then near E_F the average level spacing for this symmetry class is $\Delta = 6.266$. The numerical method introduced in [19] allows to find efficiently the billiard eigenstates and the dipole matrix elements between them (the eigenstate at the Fermi level is shown in Fig. 1). Therefore, the quantum evolution induced by a microwave field can be numerically integrated directly in the eigenbasis. This approach allows to follow the quantum excitation over thousands of microwave periods. The integration time step was set to $\Delta t = 10^{-4}$ and we ensured that its modification did not affect the excitation probabilities. In the numerical simulations the transitions below n_F were suppressed, since in a dot all states below n_F are occupied by electrons, and up to $n_{tot} = 2000$ levels above n_F were taken into account. The escape in outcome lead is modeled as absorption of all probability above the level number $n_F + n_I$ after a microwave pulse of finite duration. This corresponds to the barrier height $U = n_I\Delta$ between outcome and income leads.

Examples of probability distribution w_n over billiard eigenstates n after a long microwave pulse are shown in Fig. 2. They clearly show exponential localization of probability which can be approximately described by $w_n \sim \exp(-2n/l)/l$. The localization length in the basis n is related to the photonic length $l_\phi = l\Delta/\omega$. For large

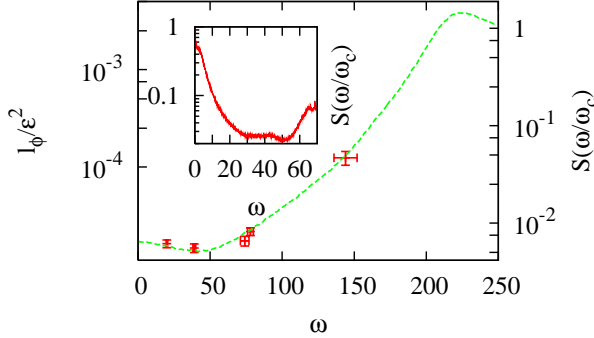


FIG. 3: (color online) Dependence of the scaled localization length l_ϕ/ϵ^2 (left axis) on the microwave frequency ω . Numerical data for $\epsilon = 1200, 1200, 1200, 600, 300$ (from left to right) are shown by points with error bars, the dashed curve shows the theory (3) with the classical spectral density $S(\omega/\omega_c)$ taken from [20]. Here $\omega_c \approx 224$, $\Delta = 6.266$. Right axis shows the scale for $S(\omega/\omega_c)$. Insert shows the dependence of classical spectral density $S(\omega)$ on ω for the three disks billiard (see text); $S(\omega)$ is given in arbitrary units and the frequency ω is adjusted to the same initial level number as in the main figure.

$\omega = 160$ the distribution shows a chain of equidistant peaks corresponding to one-photon transitions with the distance between peaks $\delta n = \omega/\Delta$. For $\omega \sim \Delta$ the peaks disappear and w_n decays in a homogeneous way.

The localization length l_ϕ can be expressed through the correlation function of dynamical motion inside the billiard. Indeed, as discussed in [20] in the semiclassical regime the dipole matrix elements of y can be expressed via the spectral density of dynamical variable $y(t)$. Using the definition of D_E and the expression for $\partial E/\partial t$ we obtain $D_E = \epsilon^2 \omega^2 R^2 S(\omega/\omega_c)/2\omega_c$. Here $\omega_c = v_F/R$ and $S(\kappa) = \lim_{T \rightarrow \infty} \left| \int_{-T}^T d\tau \xi(\tau) e^{i\kappa\tau} \right|^2 / 2T$ is the dimensionless spectral density of $\xi(\tau) = y(t)/R$ with $\tau = \omega_c t$ and $\kappa = \omega/\omega_c$. Together with (1) this result leads to

$$l_\phi = \frac{\pi \epsilon^2 R^2}{\hbar \omega_c \Delta} S(\omega/\omega_c). \quad (3)$$

In the billiard units $\omega_c = 2\sqrt{E_F}$ and for our value of E_F we have $\omega_c \approx 224$ and $l_\phi/\epsilon^2 \approx S/448$. The classical spectral density $S(\omega/\omega_c)$ has been found numerically in [20] and we show it in Fig. 3. As it is seen, $S(\omega/\omega_c)$ has one maximum with $S(1) \approx 1.8$ and it goes to a constant value $S(0) \approx 0.004$ near zero. Using (3) we can determine the quantum localization length l_ϕ from the classical value of S . Without any fit parameters this relation gives a good agreement with the numerical data of Fig. 2.

To check the theoretical dependence (3) in more detail we determine the value of l_ϕ from the fit of exponential probability decay: $\langle w_n \rangle \propto \exp(-2n\Delta/\omega l_\phi)$ (w_n is integrated in one-photon interval to extract l_ϕ). The dependence of l_ϕ/ϵ^2 on ω is shown in Fig. 3 demonstrating a good agreement with the theoretical formula (3) [21]. The dependence on ϵ at a fixed ω is shown in Fig. 4. It is

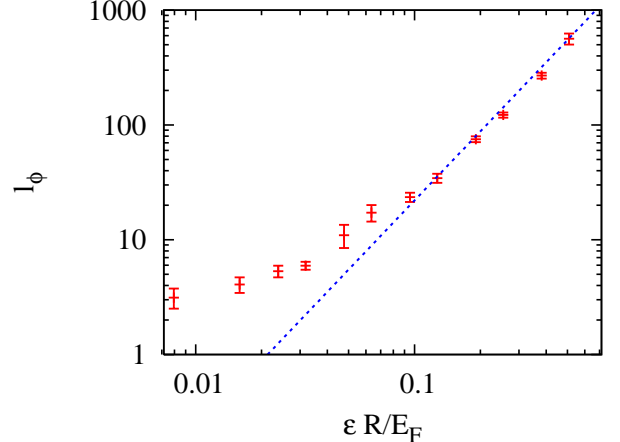


FIG. 4: (color online) Localization length l_ϕ as determined from numerical data (points) versus dimensionless field strength $\epsilon R/E_F$ for $\omega = 20$. The straight line gives the theoretical dependence (3).

also in a good agreement with the theory (3) until $l_\phi \gg 1$ which is assumed by the semiclassical approach [22].

The nontrivial property of Eq. (3) is that l_ϕ is directly dependent on the dynamical spectrum $S(\omega/\omega_c)$. For the mesoscopic billiards discussed above $\omega \ll \omega_c$ and it is interesting to have billiards with large value $S(0)$. Since $S(0)$ is simply the integrated auto-correlation function of $\xi(\tau)$, a possible choice is a billiard formed by three touching disks which exhibits a slow polynomial decay of correlations (see e.g. [23]). In Fig. 3 (insert) we show the classical power spectrum $S(\omega/\omega_c)$ versus ω for the billiard of three disks with the openings of 0.2 radian (openings are crossed by shortest straight lines which make the billiard closed). In this case the spectrum has a strong increase at small ω that gives the value of $S(0)$ by a factor 20 larger compared to the billiard of Fig. 1. The comparison of (3) with (2) gives $\chi = S(0)/4$ ($a = 2R$, $\nu_c = \pi\omega_c/2$) and for the three disks billiard we have $\chi \approx 0.02$ and $l_\phi \approx 1$ for $\epsilon = 2V/cm$ and $\mathcal{A} = \mathcal{A}_0$, $n_e = n_{e0}$.

In fact the billiard shape is of primary importance for the efficiency of microwave excitation. Indeed, a decrease of λ from $\lambda = 3/8$ to $\lambda = 0.1$ makes the unperturbed dynamics inside the billiard quasi-integrable. In the latter case a microwave field acts in an adiabatic way and the current through the dot is reduced by orders of magnitude compared to the chaotic billiard as it is shown in Fig. 5 [24]. This figure also shows that for a chaotic billiard the current through the dot is strongly reduced as soon as $\hbar\omega l_\phi$ becomes smaller than the barrier height $U = n_I \Delta$. Therefore, a conductance g between leads can be efficiently changed by varying a microwave field power. The conductance appears due to diffusion in energy which is rather similar to spatial diffusion in mesoscopic quasi-one-dimensional wires. Using analogy with the latter case where $g = E_c/\Delta$ [25], we can write the

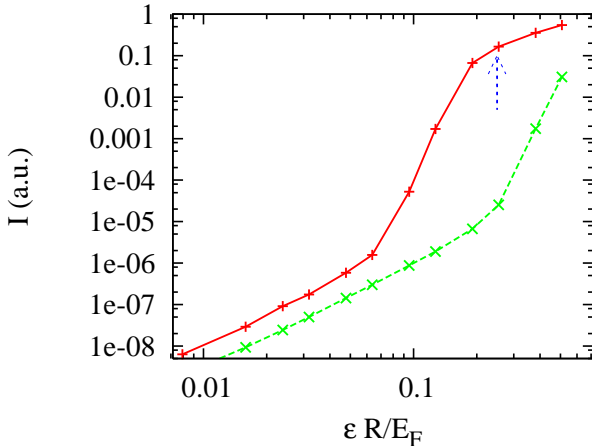


FIG. 5: Dependence of the current I through a dot billiard on a scaled microwave field strength $\epsilon R/E_F$ at $\omega = 20$, $n_F = 2001$. The current I , shown in arbitrary units, is determined as the probability on billiard eigenstates, within $2500 \leq n \leq 4000$, absorbed after a field pulse of 2000 microwave periods duration. Two curves correspond to fully chaotic billiard at $\lambda = 3/8$ (top) and to quasi-integrable billiard at $\lambda = 0.1$ (bottom). The arrow marks the position where the absorption border is reached by localization $n_I = 500 = \hbar\omega l_\phi/\Delta$.

microwave conductance of the billiard as

$$g \sim l_\phi \exp(-2N_I/l_\phi)/N_I, \quad (4)$$

where $E_c = \hbar D_E/U^2$ is the Thouless energy for diffusion in energy space, $N_I = U/\hbar\omega$ is the number of photons required to pass over the leads barrier and an effective level spacing between quasienergy levels is $\Delta_{ef} \sim \Delta/N_I$. As in [25] it drops with the sample size N_I and $g \sim E_c/\Delta_{ef}$. For $l_\phi \gg N_I$ the dot is in the metallic regime while for $l_\phi \ll N_I$ it is insulating. Thus a microwave field can efficiently switch on and off the conductance of a chaotic quantum dot blocked by a voltage difference applied between the contacts. To distinguish clearly the dependence (4) from the Arrhenius activation law at finite temperature T we need to have $T \ll \hbar\omega l_\phi$.

Of course, above we used a rather simplified model neglecting interactions between excited electrons and finite temperature of a dot. These effects destroy quantum coherence and dynamical localization and should be taken into account when comparing the theory with the experiment. However, we expect that a transition from metallic to insulating behavior induced by a microwave field (see (4)) is a robust phenomenon and thus it can be observed experimentally as it has happen with a microwave ionization of Rydberg atoms. Present experimental techniques allow to observe effects of microwave radiation on electron transport in mesoscopic dots (see e.g. [26, 27]) that makes possible experimental investigations of the effects discussed here.

We thank Kwon Ze Don for discussions which originated this work.

- [1] B. V. Chirikov, in *Chaos and Quantum Physics*, Les Houches Lecture Series **52** Eds. M.-J. Giannoni, A. Voros, and J. Zinn-Justin (North-Holland, Amsterdam, 1991), p.443.
- [2] G. Casati, B. V. Chirikov, J. Ford, and F. M. Izrailev, Lecture Notes in Physics **93**, 334 (1979).
- [3] D. L. Shepelyansky, preprint Inst. of Nucl. Phys. N. 83-61 (Novosibirsk 1983); G. Casati, B. V. Chirikov, and D. L. Shepelyansky, Phys. Rev. Lett. **53**, 2525 (1984).
- [4] E. J. Galvez, B. E. Sauer, L. Moorman, P. M. Koch, and D. Richards, Phys. Rev. Lett. **61**, 2011 (1988).
- [5] J. E. Bayfield, G. Casati, I. Guarneri, and D. W. Sokol, Phys. Rev. Lett. **63**, 364 (1989).
- [6] M. Arndt, A. Buchleitner, R. N. Mantegna, and H. Walther, Phys. Rev. Lett. **67**, 2435 (1991).
- [7] H. Maeda, and T.F.Gallagher, Phys. Rev. Lett. **93**, 193002 (2004).
- [8] F. L. Moore, J. C. Robinson, C. F. Bharucha, B. Sundaram, and M. G. Raizen, Phys. Rev. Lett. **75**, 4598 (1995).
- [9] N.B.Delone, V.P.Krainov, and D.L.Shevelyansky, Sov. Phys. Uspekhy **26**, 551 (1983).
- [10] Th. Zimmermann, L. S. Cederbaum, H.-D. Meyer, and H. Köppel, J. Phys. Chem. **91**, 4446 (1987).
- [11] H. Friedrich, and D. Wintgen, Phys. Rep. **1983**, 37 (1989).
- [12] I. P. Kornfeld, S. V. Fomin, and Ya. G. Sinai, *Ergodic theory*, Springer, Berlin, 1982.
- [13] O. Bohigas, M. J. Giannoni, and C. Schmit, Phys. Rev. Lett. **52**, 1 (1984).
- [14] M. V. Berry, and M. Robnik, J. Phys. A **19**, 1365 (1986).
- [15] D.Shevelyansky, Physica D **28**, 103 (1987).
- [16] G.Benenti, G.Casati and D.L.Shevelyansky, Eur. Phys. J. D **5**, 311 (1999).
- [17] C. W. J. Beenakker, Rev. Mod. Phys. **69**, 731 (1997).
- [18] Y.Alhassid, Rev. Mod. Phys. **72**, 895 (2000).
- [19] M. Robnik, J. Phys. A **16**, 3971 (1983); *ibid* **17**, 1049 (1984).
- [20] T. Prosen and M. Robnik, J. Phys. A **26**, L319 (1993); T. Prosen, Ann. Phys. (NY), **235**, 115 (1994).
- [21] Eq. (3) assumes that the energy excitation $\hbar\omega l_\phi$ remains small compared to E_F , at large ω it gives a noticeable fraction of E_F that leads to horizontal error bars in Fig. 3.
- [22] Also the size of field oscillations should be larger than the wavelength implying $\epsilon/(m\omega^2) > R/n_F^{1/2}$.
- [23] R. Artuso, G. Casati, and I. Guarneri, Phys. Rev. E **51**, R3807 (1995).
- [24] While in experiments it may be not easy to vary directly a dot shape, it may be possible to introduce a magnetic field which should make the dynamics quasi-integrable as soon as the Larmor radius becomes much smaller than the dot size. For a dot with parameters A_0 and n_{e0} discussed above this corresponds to a magnetic field $B \sim 1T$.
- [25] D. J. Thouless, Phys. Rev. Lett. **39**, 1167 (1977).
- [26] A.A. Bykov, G.M. Gusev, Z.D.Kvon, D.I.Lubyshev, and V.P.Migal', JETP Lett. **49**, 13 (1989).
- [27] R. Deblock, Y. Noat, B. Reulet, H. Bouchiat, and D. Mailly, Phys. Rev. B **65**, 075301 (2002).